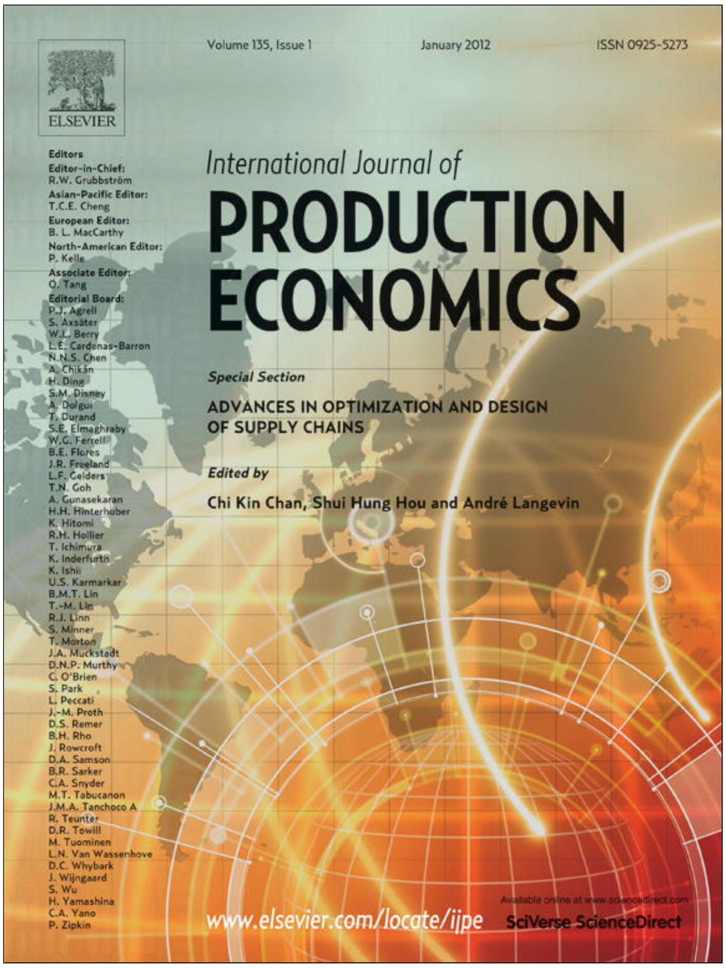
Volume 135, Issue 1
January 2012
ISSN 0925-5273
ELSEVIER
International Journal of
PRODUCTION ECONOMICS
Special Section
ADVANCES IN OPTIMIZATION AND DESIGN OF SUPPLY CHAINS
Edited by
Chi Kin Chan, Shui Hung Hou and André Langevin
www.elsevier.com/locate/ijpe
SciVerse ScienceDirect

Int. J. Production Economics 135 (2012) 479–490

Contents lists available at SciVerse ScienceDirect

Int. J. Production Economics

journal homepage: www.elsevier.com/locate/ijpe

A comparison study of effectiveness and robustness of control charts for monitoring process mean

Yanjing Ou [a], Zhang Wu [a,*], Fugee Tsung [b]

[a] School of Mechanical and Aerospace Engineering, Nanyang Technological University, Singapore 639798, Singapore
[b] Department of Industrial Engineering and Logistics Management, Hong Kong University of Science and Technology, Hong Kong

ARTICLE INFO

Article history:
Received 4 October 2010
Accepted 22 August 2011
Available online 7 September 2011

Keywords:
Quality control
Statistical process control
Control charts
Variable sample sizes and sampling intervals (VSSI)
Robust design

ABSTRACT

This article compares the effectiveness and robustness of nine typical control charts for monitoring the mean of a variable, including the most effective optimal and adaptive Sequential Probability Ratio Test (SPRT) charts. The nine charts are categorized into three types (the $\bar{X}$ type, CUSUM type and SPRT type) and three versions (the basic version, optimal version and fully adaptive (FA) version). While the charting parameters of the basic charts are determined by common wisdoms, the parameters of the optimal and fully adaptive charts are designed optimally in order to minimize an index, Average Extra Quadratic Loss (*AEQL*), for the best overall performance. A Performance Comparison Index, *PCI*, is also proposed as the measure of the relative overall performance of the charts. This comparison study does not only compare the detection effectiveness of the charts, but also investigate their robustness in performance. Moreover, the probability distribution of the mean shift δ is studied explicitly as an influential factor in a factorial experiment. Apart from many other findings, the results of this study reveal that the SPRT chart is more effective than the CUSUM chart and $\bar{X}$ chart by 58% and 126%, respectively, from an overall viewpoint. Moreover, it is found that the optimization design of charting parameters can increase the detection effectiveness by 29% on average, and the adaptive features can further enhance the detection power by 35%. Finally, a set of design tables are provided to facilitate the users to select a chart for their applications.

1. Introduction

Since it was introduced as a Statistical Process Control (SPC) tool to monitor processes and ensure quality, the control chart has been increasingly adopted in modern industries and non-manufacturing sectors. More and more new charts have been developed over the decades and recently (Magalhães et al., 2009; Costa and Machado, 2011; Zhou and Lian, 2011; Wu et al., 2011; Celano et al., 2011). It is essential to have a systematic study that evaluates and compares the performance of different charts in a quantitative and analytical manner under various conditions, so that the SPC users not only roughly know which charts are better than the others, but are also aware of the degree of difference in performance among the charts. This kind of information will greatly facilitate the SPC users to select a suitable chart for their applications. Usually, a user may not be interested to adopt a complicated chart just for a performance improvement of 1–2%. But if the achievable improvement resulting from an advanced chart is more than, say 20%, he will be willing to make effort and spend resources to adopt the advanced chart. In addition to chart effectiveness (the detection speed), the users may also be concerned with the robustness of the charts, that is, whether the performance of a chart is stable under different conditions compared with the leading charts. The probability distribution of mean shift δ will be different in different process. Its influence on the chart performance should also be investigated carefully.

Some comparison studies of chart performance are available in literature, including the comparisons of the multivariate EWMA charts (Margavio and Conerly, 1995), the adaptive $\bar{X}$, CUSUM charts and a special SPRT chart (Stoumbos and Reynolds, 2001), the economic control charts (Tannock, 1997), the Shewhart and CUSUM charts for monitoring process of mean and variance (Reynolds and Stoumbos, 2004a), the non-parametric charts for detecting defect shifts (Das, 2009), the profile monitoring approaches (Colosimo and Pacella, 2010), the GLR chart (Reynolds and Lou, 2010) and the CUSUM charts for detecting mean shifts (Wu et al., 2009; Ryu et al., 2010) or both mean and variance shifts (Wu et al., 2010).

However, few of the comparative studies have covered all major types and versions of the control charts for monitoring process mean. Specifically, seldom are the very effective SPRT charts and adaptive charts included. Many of these studies are conducted in a qualitative or descriptive manner. Such qualitative

* Corresponding author. Tel.: +65 67904445; fax: +65 67911859.
E-mail address: mzwu@ntu.edu.sg (Z. Wu).

0925-5273/$ - see front matter © 2011 Elsevier B.V. All rights reserved.
doi:10.1016/j.ijpe.2011.08.026

approaches are unable to tell the degree of the superiority of one chart over another or to rank the charts' performance properly when several charts are involved in the comparison. Moreover, almost none of these comparisons has either considered the robustness of chart performance or the probability distributions of the mean shift δ. In most of the studies, the charting parameters have not been optimized, that is, a chart used for comparison may not be the best one of its type and version.

This article studies the overall performance of nine typical control charts for monitoring process mean in a quantitative and analytical manner. It includes the $\overline{X}$ type, CUSUM type and SPRT type charts, and three versions (the basic version, optimal version and fully adaptive or FA version) for each type. While the basic and optimal charts use fixed sample size and sampling interval (FSSI), the FA charts vary the sample sizes n and sampling intervals d according to the observed data from the process. The FA chart is the most effective adaptive chart as it adapts both n and d. In this study, while the FA versions of the $\overline{X}$ and CUSUM charts adopt the Variable Sample Sizes and Sampling Intervals (VSSI) model, the FA SPRT chart will use the Variable Sampling Intervals (VSI) model, because the SPRT chart has incorporated adaptive sample size feature intrinsically.

The optimal and FA charts will be designed by an optimization procedure in which the objective function to be minimized is the Average Extra Quadratic Loss (*AEQL*). The index *AEQL* is actually a weighted average Average Time to Signal (*ATS*) and works as a measure of the overall performance of the charts. In addition to detection effectiveness, the performance robustness or stability will also be investigated. A factorial experiment will use a quantitative approach to compare the nine charts under different specifications on false alarm rate and mean shift range. Moreover, the probability distribution of the mean shift δ will also be handled explicitly as an input factor. The main findings obtained in this study include: (1) the SPRT chart is more effective than the CUSUM chart and $\overline{X}$ chart by 58% and 126%, respectively, from an overall viewpoint; (2) the optimization design of the charting parameters can increase the detection effectiveness by 29% on average, and it can further increase the power by 35% if enhanced by the adaptive feature; (3) using either *AEQL* or Average Ratio of *ATS* (*ARATS*) as the measure, the overall performance ranking of the charts is found identical in general; (4) the more effective charts also have more robust or stable performance under different conditions; (5) the optimal CUSUM chart is the most effective and robust fixed sample size and sampling interval (FSSI) chart and the optimal SPRT chart is the best choice among the adaptive charts and (6) the optimal sample sizes $n_{\overline{X}}$ of the $\overline{X}$ charts often fall beyond the conventional range between 4 and 6, and the optimal sample sizes n_{CUSUM} of the CUSUM charts is often larger than one. These results and findings, together with a set of design tables, will provide the SPC users with useful aids to select and design a suitable chart for their application.

The focus of this study is the monitoring of process mean μ. In SPC for variables, the monitoring of μ is an important issue and has attracted much research effort (Reynolds and Lou, 2010; Ryu et al., 2010). In fact, in many current SPC applications, only the process mean is monitored by a control chart. More importantly, many new techniques and methodologies developed for mean monitoring can be modified and then applied to the monitoring of both mean and variance of a variable.

Without loss of generality, only the upper-sided control charts for detecting increasing mean shifts ($\delta > 0$) are discussed in detail in this article. The lower-sided charts for detecting decreasing mean shifts have symmetrical structures and identical operating characteristics relative to the upper-sided charts. Moreover, only sustained process shifts are studied as they are probably more common and most practitioners would probably give higher priority to detecting them (Reynolds and Stoumbos, 2004a).

In this study, the quality characteristic x is assumed to follow an identical and independent normal distribution with known in-control μ_0 and standard deviation σ_0 (μ_0 and σ_0 may be estimated from the field records or historical data). It is also assumed that σ is constant, i.e., $\sigma \equiv \sigma_0$. A process shift makes the process mean μ change from μ_0 to $\mu_0 + \delta\sigma_0$ (δ is the mean shift in terms of σ_0 and called the standardized mean shift). For the convenience of discussion, x will be converted to z which follows a standard normal distribution when process is in control.

$$z = \frac{x - \mu_0}{\sigma_0} \tag{1}$$

The in-control and out-of-control performances of a control chart is usually measured by the Average Time to Signal (*ATS*). The in-control ATS_0 must be large enough so that false alarm occurs infrequently. On the other hand, the out-of-control *ATS* should be short enough in order to detect the process shifts quickly. In this study, the out-of-control *ATS* is computed under the steady-state mode. It assumes that the process has reached its stationary distribution at the time when the process shift occurs.

The remainder of the article proceeds as follows. The nine control charts will be introduced in the next section, followed by the discussion of the general methodologies of the comparative study. The chart performance will be first compared for a general case, and then further studied in a factorial experiment. Subsequently, the design tables are introduced, and an illustrative example is presented. The discussions and conclusions are drawn in the last section.

2. Nine control charts

It is impossible to include all the control charts with different types and versions in any comparative study. In this study, nine typical and representative charts will be investigated. They are categorized into three types ($\overline{X}$, CUSUM and SPRT) and three versions (basic, optimal, fully adaptive or FA).

	Basic	Optimal	Fully adaptive
$\overline{X}$	Basic $\overline{X}$	Optimal $\overline{X}$	VSSI $\overline{X}$
CUSUM	Basic CUSUM	Optimal CUSUM	VSSI CUSUM
SPRT	Basic SPRT	Optimal SPRT	VSI SPRT

Each type or version has distinctive level of performance and different ways for implementation. The $\overline{X}$ type charts (Shewhart, 1931) decide process status based on the observations in the latest sample. The CUSUM type charts (Page, 1954) consider the data in all sample points by checking the cumulative sum. The EWMA type charts also utilize the cumulative information in a series of samples. However, they are not included in this study as their performance is quite similar to that of the CUSUM type charts (Reynolds and Stoumbos, 2004b). The SPRT charts are developed based on the sequential probability ratio test (Wald, 1947). A typical model of the SPRT chart proposed by Stoumbos and Reynolds (1997) will be employed in this article. This SPRT chart allows the sample size to vary based on the data observed at the current sample. Its statistical properties are evaluated based on an assumption that the time required to obtain an individual observation is short enough to be neglected, relative to the sampling interval.

The basic version of each type of charts serves as the baseline for the comparison and its charting parameters are determined according to common wisdoms and conventions. Contrarily, the parameters of the optimal and FA charts will be determined analytically aiming at the best overall performance.

Each control chart is designed subject to two constraints related to the inspection rate and false alarm rate. The inspection rate is equal to the ratio between the average sample size and the average sampling interval. The resultant or actual inspection rate (r_0) must be no larger than the allowed inspection rate (R), i.e.,

$$r_0 \le R. \tag{2}$$

Moreover, the in-control ATS_0 must be made equal to or larger than a specified value (τ) that depends on the requirement on false alarm rate.

$$ATS_0 \ge \tau. \tag{3}$$

Some introductions to the design and implementation of each of the nine charts are given below:

(1) **The basic $\overline{X}$ chart**: This chart has three parameters: the sample size n, sampling interval d and control limit H. According to the common practice in SPC, the sample size n usually takes a value between four and six (Montgomery, 2009). In this study, n is set at five. The sampling interval d depends on the allowed inspection rate (constraint (2)), and the control limit H is decided by the required false alarm level (constraint (3)).

(2) **The optimal $\overline{X}$ chart**: This chart also has three parameters n, d and H. However, its sample size n, as an independent design variable, will be determined by an optimization design. Other two parameters d and H are treated as dependent variables and still determined by the two constraints (2) and (3).

(3) **The VSSI $\overline{X}$ chart**: This chart has six parameters: the sample size n_1 and n_2 ($n_1 < n_2$), sampling interval d_1 and d_2 ($d_1 > d_2$), warning limit w and control limit H ($w < H$). Firstly, as recommended by many researchers (Runger and Montgomery, 1993), the shorter sampling interval d_2 is fixed at a minimum allowable value (d_{min}). Then the sample sizes n_1, n_2 and the longer sampling interval d_1 are taken as the independent design variables and are determined by an optimization search. The warning limit w and control limit H are determined by constraints (2) and (3), respectively. During implementation, if $\bar{z} \le w$ ($\bar{z}$ is the sample mean of the standardized x), the smaller sample size n_1 and longer sampling interval d_1 are employed for the next sample, otherwise n_2 and d_2 are in use. Different warning limits could be used for adapting the sample sizes and sampling intervals. However, only one warning limit is being used in most studies, because it is relatively easier to be designed and implemented and may gain most of the benefits that can be reached by an adaptive chart (Zhang and Wu, 2006).

(4) **The basic CUSUM chart**: This chart has four parameters: n, d, H and reference parameter k. According to the recommendation in most papers (Reynolds and Stoumbos, 2004a), the sample size n is set as one, because ($n=1$) makes the CUSUM chart much more sensitive to large process shifts and, therefore, more effective from an overall viewpoint. In this study, the reference parameter k is set at 0.5 for $\delta_{max} \le 3.5$, at 0.8 for $3.5 < \delta_{max} \le 5$, and at 1.2 for $\delta_{max} > 5$, where δ_{max} is the maximum mean shift. The sampling interval d and control limit H are determined by the two constraints. An upper-sided CUSUM chart keeps on examining the cumulative sum C_t.

$$C_0 = 0,$$
$$C_t = \max(0, C_{t-1} + \overline{Z} - k). \tag{4}$$

When $C_t > H$, the process is thought out of control.

(5) **The optimal CUSUM chart**: This chart also has four parameters n, d, k and H. The sample size n and reference parameter k will be determined by an optimization search.

(6) **The VSSI CUSUM chart**: This chart has seven parameters: n_1, n_2, d_1, d_2, k, w and H. The shorter sampling interval d_2 is fixed at d_{min}. The independent variables n_1, n_2, d_1 and k will be determined optimally. The warning limit w and control limit H are determined by constraints (2) and (3), respectively.

(7) **The basic SPRT chart**: This chart has four parameters: the sampling interval d, reference parameter k, lower control limit g and upper control limit H ($g < H$). To design a basic SPRT chart, an operating characteristic Average Sample Number (ASN) also has to be determined. It is actual the average sample size of the SPRT chart. For the basic SPRT chart, ASN is set as 3 and k as 0.15 with reference to the cases and examples presented in Stoumbos and Reynolds (1997). The sampling interval d is determined by the inspection rate, i.e.,

$$d = ASN/R. \tag{5}$$

Finally, the two control limits g and H are adjusted simultaneously so that constraints (2) and (3) are satisfied. When taking a sample of an upper-sided SPRT chart, the observation z_i is taken sequentially and the cumulative sum C_i is examined.

$$C_0 = 0,$$
$$C_i = C_{i-1} + z_i - k. \tag{6}$$

If $C_i > H$, the process is considered out of control. If $g \le C_i \le H$, sampling will be continued. Finally, if $C_i < g$, the process is considered in control and the current sampling is terminated.

(8) **The optimal SPRT chart** (Ou et al., 2011a, b): This chart also has four parameters d, k, g and H. The sampling interval d and reference parameter k will be optimized.

(9) **The VSI SPRT chart** (Ou et al., 2011a, b): This chart has six parameters: d_1, d_2, k, w, g and H. The independent variables d_1, d_2, k and w will be determined optimally. The dependent variables g and H are determined so that constraints (2) and (3) are satisfied. During implementation, if the sample mean $\bar{z}$ of a sample is smaller than w, the longer sampling interval d_1 is adopted for the next sample, otherwise d_2 is to be used. The sample size used to calculate $\bar{z}$ is a random variable rather than a constant.

While the ATS values of the $\overline{X}$ chart can be calculated by simple formulae, the ATS values of the CUSUM and SPRT charts are evaluated by the Markov procedure. The detailed procedure for the SPRT charts (including the VSI SPRT chart) can be found in Ou et al. (2011a, b).

3. Methodologies of the investigation

3.1. Specifications

To carry out the design of a control chart, all or part of the following four specifications have to be determined:

(1) The allowed inspection rate (R). The value of R depends on the available resources such as manpower and instrument. Usually, only the in-control (or long run) value of R is considered, because a process often runs in an in-control condition for a long period and only occasionally falls into an out-of-control status for a short time period. The inspection rate in the short out-of-control period has little influence on the long run value of R and is of much less concern (Arnold and Reynolds, 2001).

(2) The minimum allowable value (τ) of the in-control ATS_0. The value of τ is decided based on the requirement on false alarm rate.
(3) The maximum value (δ_{max}) of the mean shift δ. The value of δ_{max} may be determined based on the knowledge about a process (e.g., the maximum possible mean shift in a process) or on the shift range the users are interested to investigate. The optimal values of the reference parameter k of the CUSUM and SPRT charts usually increase along with the increase of δ_{max}.
(4) The minimum allowable value (d_{min}) of sampling interval d. The value of d_{min} is determined by some practical considerations, such as the amount of inspection that can be finished in a short time period or the assumption for a SPRT chart that d must be significantly larger than the time for taking an observation.

In this study, the time unit is made equal to the time period in which the available resource allows one unit (or one product) to be inspected. For example, if the available resource allows five units to be inspected per hour, the time unit is 12 (=60/5) min. This setting has a benefit that the inspection rate R always equals one. It only influences the scaling of the sampling interval d, but has no effect on the results of comparison (noted, in the above example, the actual time t required to inspect a unit is smaller, or much smaller, than the standard time unit (12 min). That is, an operator will spend only t min to conduct inspection and the remaining (12—t) minutes to carry out other operation in each standard time unit).

In this study, the minimum sampling interval d_{min} is fixed at 0.3 in terms of the standard time unit. As R and d_{min} are fixed, only two remaining specifications τ and δ_{max} have to be determined.

3.2. Performance measures

Since it is quite difficult to predict the values of process shifts in most applications, therefore, it is very important that a control chart has good performance over the whole process shift range rather than just for a specific mean shift (Sparks, 2000; Reynolds and Stoumbos, 2004a; Shu and Jiang, 2006; Wu et al., 2008). A sound measure of overall effectiveness is the Average Extra Quadratic Loss ($AEQL$) based on the quadratic loss function (Taguchi and Wu, 1980) which is widely used as a design criterion by many authors (Chou et al., 2000; Reynolds and Stoumbos, 2004b; Zhang and Wu, 2006; Chen and Chen, 2007; Serel and Moskowitz, 2008). The index $AEQL$ can be calculated by the following formula (Wu et al., 2004; Reynolds and Stoumbos, 2004b; Ryu et al., 2010).

$$AEQL = \int_{\delta_{\min}}^{\delta_{\max}} \delta^2 ATS(\delta) f_\delta(\delta) d\delta. \tag{7}$$

where $f_\delta(\delta)$ is the probability density function of mean shift and $ATS(\delta)$ is the ATS value resulted from a mean shift δ. The method of Legendre–Gauss Quadrature can be used to compute the integration quickly and accurately. It is noted that $AEQL$ is a weighted average ATS using the square of mean shift (δ^2) as the weight. This weight can be justified as quality is inversely proportional to variability (Montgomery, 2009). If a chart has a small $AEQL$ value, its out-of-control ATS value over the entire shift range is low, on average.

The use of δ_{min} ($\delta_{min}>0$) in Eq. (7) may help to avoid over-correction against minor shifts. However, since the portion from zero to δ_{min} usually makes little contribution to the entire integration of $AEQL$ due to the weight of δ^2, δ_{min} is set as zero in this study for simplicity. Then, Eq. (7) can be rewritten as

$$AEQL = \int_{0}^{\delta_{\max}} \delta^2 ATS(\delta) f_\delta(\delta) d\delta, \tag{8}$$

In practice, it is very difficult, if not impossible, to estimate the probability distribution of δ, because the data of out-of-control cases are not only sparse, but also become obsolete when the assignable causes are identified and removed. As a result, it is generally assumed explicitly (Domangue and Patch, 1991; Sparks, 2000; Wu et al., 2009) or implicitly (Reynolds and Stoumbos, 2004a, *b*) that all process shifts occur with equal probability, and a uniform distribution with a density function of ($1/\delta_{max}$) is used for δ. Consequently, Eq. (8) can be further simplified as follows:

$$AEQL = \frac{1}{\delta_{\max}} \int_{0}^{\delta_{\max}} \delta^2 ATS(\delta) d\delta. \tag{9}$$

In this article, $AEQL$ is mainly calculated by the above formula or based on the uniform distribution assumption. A discussion regarding the influence of the non-uniform distributions of δ on the $AEQL$ value will be presented in the next section.

Another index, Average Ratio of ATS ($ARATS$), is probably a more heuristic measure of the overall performance. It directly calculates the average of the ratios between the out-of-control $ATS(\delta)$ of a chart to be evaluated and the $ATS(\delta)_{benchmark}$ of a benchmark chart.

$$ARATS = \frac{1}{\delta_{\max}} \int_{0}^{\delta_{\max}} \frac{ATS(\delta)}{ATS(\delta)_{benchmark}} d\delta \tag{10}$$

The chart producing smallest average ATS is usually selected as the benchmark. By this way, the $ARATS$ values of all charts will be equal to or larger than one, and the value of ($ARATS$ -1) directly indicates the degree of inferiority of a chart compared with the benchmark chart.

In this study, $AEQL$ will be used as the objective function for the optimization designs of the control charts, because the computation of $AEQL$ does not require a predetermined benchmark chart and therefore is relatively more tractable. Furthermore, the use of $AQEL$ can avoid some possible bias incurred by the selection of the benchmark.

3.3. Optimization model

Based on the specifications, the charting parameters of the optimal and FA charts will be determined by the following optimization model:

$$\text{Objective function}: AEQL = \text{minimum}, \tag{11}$$

$$\text{Constraint functions}: ARL_0 = \tau, \tag{12}$$

$$r_0 = R, \tag{13}$$

Independent or dependent design variables:Charting parameters.

As discussed in the last section, different control charts use different charting parameters as the independent or dependent design variables. The optimal values of the independent design variables are searched so that the objective function $AEQL$ is minimized. Any nonlinear programming can be used to search the optimal solution. The dependent design variables are adjusted to meet the two constraints (12) and (13). The two constraints are treated as equality constraints rather than inequality ones. This helps to make full use of the available resources and chart capacity. In actual computer coding, they are implemented as

$$|ARL_0 - \tau| < 1, |(r_0 - R)/R| < 0.005. \tag{14}$$

In the optimization designs, an optimal combination of sample size and sampling interval is usually searched under the constraint on inspection rate. This seems to violate the rational subgroups concept. However, due to the increasing demands on high quality products, the increase of production rate and the wide applications of on-line measurement and distributed computing systems in today's SPC (Woodall and Montgomery, 1999), sampling frequency becomes higher and sampling intervals may be much smaller than the working shifts. As a result, the concept of rational subgroups becomes less effective. It is especially true for CUSUM and SPRT charts (Hawkins and Olwell, 1998). In fact, when researchers (Reynolds and Stoumbos, 2004a) investigated the best combination of sample size and sampling interval for a control chart, they always disregarded the rational subgroups concept.

4. A general case

The nine control charts are first compared for a general case in which specifications are set as below:

$$\tau = 740, \delta_{\max} = 4. \quad (15)$$

It is recalled that other two specifications for inspection rate R and minimum sampling interval d_{min} are fixed as (R=1) and (d_{min}=0.3).

The nine charts are designed based on this set of specifications and the charting parameters are listed in Table 1. The *ATS* values of the charts are calculated within the mean shift range from zero to δ_{max} (=4.0), and also displayed in Table 1. The curve of the normalized *ATS* (i.e., $ATS/ATS_{VSI\ SPRT}$) versus δ is illustrated in Fig. 1.

From both Table 1 and Fig. 1, it is observed that the difference between the *ATS* values of the nine charts is very substantial. The curves in Fig. 1 reveal that the SPRT type charts (in Fig. 1(*c*)) significantly outperform the CUSUM type charts (in Fig. 1(*b*)), and the latter are substantially more effective than the $\overline{X}$ type charts (in Fig. 1(*a*)). On the other hand, within each type of charts, the FA version outperforms the optimal version which in turn surpasses the basic version from an overall viewpoint. For most of the cases, a chart is unable to produce smaller *ATS* than other

Table 1
ATS values of the nine charts (τ=740, δ_{max}=4).

	Basic $\bar{x}$	Optimal $\bar{x}$	VSSI $\bar{x}$	Basic CUSUM	Optimal CUSUM	VSSI CUSUM	Basic SPRT	Optimal SPRT	VSI SPRT
	n_1=5 d_1=5.0000 H=1.1046	n_1=3 d_1=3.0000 H=1.5286	n_1=2 n_2=2 d_1=2.4419 d_2=0.3000 w=0.5762 H=1.9666	n_1=1 d_1=1.0000 k=0.8000 H=3.1405	n_1=2 d_1=2.0000 k=0.6838 H=1.5917	n_1=1 n_2=2 d_1=1.3419 d_2=0.3000 k=0.5500 w=0.8769 H=3.0916	d_1=3.0000 k=0.1500 g=0.4651 H=10.8355 ASN=3.0010	d_1=1.3419 k=0.4500 g=0.6928 H=5.0004 ASN=1.3425	d_1=1.3919 d_2=0.6419 k=0.4000 g=0.8790 w=0.7243 H=5.3416 ASN=1.2909
δ									
0.0	740	740	740	740	740	740	740	739	740
0.4	84.4	117	119	82.2	70.7	39.0	13.7	32.3	30.5
0.8	17.7	27.5	23.2	17.5	15.2	6.61	4.87	5.50	5.43
1.2	6.05	9.04	5.95	6.96	6.34	3.05	2.91	2.33	2.29
1.6	3.27	3.96	2.40	3.95	3.70	1.95	2.14	1.41	1.36
2.0	2.62	2.28	1.56	2.68	2.51	1.43	1.78	1.02	0.98
2.4	2.51	1.71	1.31	2.00	1.84	1.15	1.62	0.83	0.81
2.8	2.50	1.54	1.23	1.59	1.42	0.98	1.54	0.74	0.73
3.2	2.50	1.51	1.20	1.31	1.17	0.87	1.51	0.70	0.69
3.6	2.50	1.50	1.19	1.10	1.05	0.80	1.50	0.68	0.68
4.0	2.50	1.50	1.19	0.92	1.01	0.74	1.50	0.67	0.67
AEQL	16.5153	13.8385	11.0411	11.5658	10.6298	6.6370	9.0738	5.2821	5.1795
PCI	3.1886	2.6718	2.1317	2.2330	2.0523	1.2814	1.7519	1.0198	1.0000
ARATS	3.0001	2.8427	2.2442	2.4054	2.1943	1.3019	1.5927	1.0229	1.0000

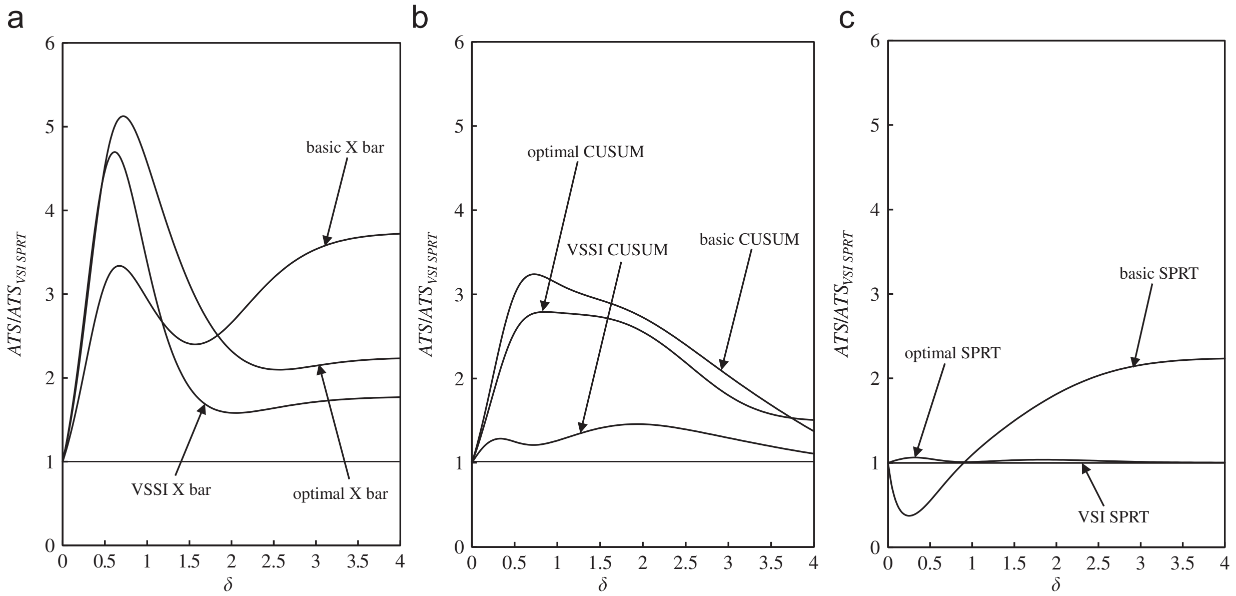

Fig. 1. Normalized *ATS* ($ATS/ATS_{VSI\ SPRT}$).

charts at all shift points or values (Reynolds and Stoumbos, 2006). However, as long as one chart has smaller *ATS* at more points and/or to a larger degree, this chart is thought to be more effective than others. It is noted that, the VSI SPRT chart almost always produces the lowest *ATS* across the entire mean shift range compared with other charts, except that it is less sensitive to very small δ (i.e., $\delta < 0.9$) than the basic SPRT chart (see Fig. 1(*c*)). The *ATS* of the VSI SPRT chart may be several times smaller than the *ATS* of the $\overline{X}$ and CUSUM charts. However, the superiority of the VSI SPRT chart over the optimal SPRT chart is minor.

The values of the two overall performance indices *AEQL* (Eq. (9)) and *ARATS* (Eq. (10)) are also shown in Table 1, together with another index, Performance Comparison Index (*PCI*). The index *PCI* is the ratio between the *AEQL* of a chart and the *AEQL* of the best chart under the same conditions (i.e., the same specified values of τ and δ_{max}, as well as the same probability distribution of δ that will be discussed shortly). This index facilitates the performance comparison and ranking based on *AEQL*. The chart with the lowest *AEQL* has a *PCI* value equal to one, and the *PCI* values of all other charts are larger than one. Since the VSI SPRT chart has the smallest *AEQL* in this general case, it stands as the best chart and

$$PCI = \frac{AEQL}{AEQL_{best\ chart}} = \frac{AEQL}{AEQL_{VSI\ SPRT}}. \tag{16}$$

The VSI SPRT chart is also used, in this general case, as the benchmark for calculating *ARATS* in Eq. (10). These three indices, *AEQL*, *ARATS* and *PCI*, provide fairly comprehensive information regarding the comparison of the overall performance of the charts.

If the nine charts are to be ranked from the most effective one to the least effective one for this general case, it is interesting to find that the ranking based on *PCI* and *ARATS* are exactly the same as below

$$\text{VSI SPRT, optimal SPRT, VSSI CUSUM, basic SPRT, optimal CUSUM,}$$
$$\text{VSSI } \overline{X}\text{, basic CUSUM, optimal } \overline{X}\text{, basic } \overline{X} \text{ chart.} \tag{17}$$

This is an evidence that the above ranking is reasonable and trustful. Since both *PCI* and *ARATS* usually deliver the similar results about the relative performance of the charts, only *PCI* will be pursued in the following discussions.

From the ranking in Eq. (17), it is noted that, without the optimization design, a SPRT chart may be less effective than a VSSI CUSUM chart and a CUSUM chart may be less effective than a VSSI $\overline{X}$ chart.

It is noteworthy that, in all above discussions, *AEQL* is determined by Eq. (9) which implies that the mean shift δ follows a uniform distribution. In practice, the distribution of δ is likely to be non-uniform. However, since it is very difficult to estimate this probability distribution, one may have to design the control charts based on a uniform distribution assumption.

A concern arises how well these charts will work and compare with each other if the actual distribution of δ is quite different from a uniform one. A test is carried out on the nine charts for the general case in this section. It is noted that all these charts are designed based on the assumption of uniform distribution. Now they are applied to three different cases or processes. In each case, the mean shift δ follows a beta probability distribution with the following density function:

$$f_\delta(\delta) = \frac{\Gamma(a+b)}{\Gamma(a)\Gamma(b)} \frac{\delta^{a-1}(\delta_{\max}-\delta)^{b-1}}{(\delta_{\max})^{a+b-1}} \tag{18}$$

The three beta distributions serve as the representatives of different types of non-uniform probability distributions of δ (Fig. 2). The skewness of a beta distribution depends on the

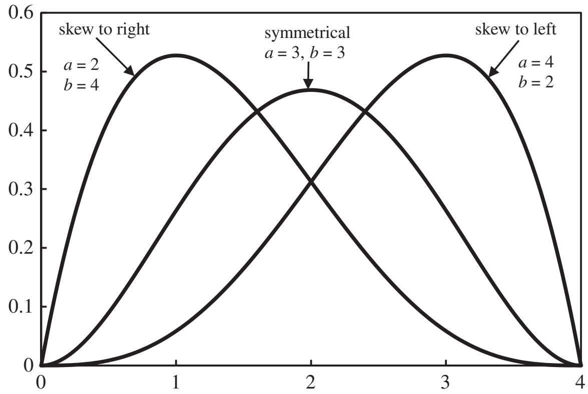

Fig. 2. Three Beta distributions.

parameters *a* and *b*. If $(a<b)$, δ has a probability distribution skewed to right. This represents the situations where most of the shifts cluster to the lower end within the shift range. If $(a>b)$, δ has a probability distribution skewed to left. Finally, if $(a=b)$, δ has a symmetrical probability distribution. With a given probability distribution $f_\delta(\delta)$, the *AEQL* produced by a control chart is calculated by the general formula (Eq. (8)) rather than the uniform formula (Eq. (9)).

Now each of the nine control charts that were designed based on the uniform assumption (their charting parameters are listed in Table 1) is applied to three processes with different $f_\delta(\delta)$ as shown in Fig. 2. That is, the *AEQL* value is calculated by Eq. (8). The resultant *AEQL* values under the three beta distributions, as well as the *AEQL* values under the uniform distribution, are displayed in the top half of Table 2. As expected, the *AEQL* values produced by all nine charts become smaller when the probability distribution $f_\delta(\delta)$ is skewed to right, and they become larger when $f_\delta(\delta)$ is skewed to left. The bottom half of Table 2 shows the *PCI* (the ratio of $AEQL/AEQL_{\text{best}}$) values for each case (or under each column for a particular distribution). For example, each *PCI* value under the column "skew to right" is obtained by dividing each *AEQL* value under that column by the *AEQL* value of the VSI SPRT chart that also appears under that column, as the VSI SPRT chart has the smallest *AEQL* value (3.9259) for the beta distribution that is skew to right. Consequently, a *PCI* value indicates the *AEQL* value of a chart relative to the *AEQL* value of the best chart when both charts are designed under the same τ and δ_{max} and applied to the process with the same $f_\delta(\delta)$. The rightmost column in the bottom half of Table 2 displays the average *PCI* of a chart over three different beta distributions.

The numbers inside the parentheses in the bottom half of Table 2 indicate the rankings of the *PCI* values in each column. It is found that the ranks in each column are quite similar to the ranking under the uniform assumption with only one exchange of chart ranking positions under the three columns of "symmetrical", "skew to left" and "average", and two exchanges under the column of "skew to right". Specifically, the *PCI* value of each chart under column of "uniform" is quite close to its counterparts under the columns of "symmetrical" and "average". This implies that, if a chart is designed using a uniform assumption, the relative performance of this chart (or its ranking position) will be nearly the same if the actual distribution of δ is either uniform or symmetrical. Furthermore, if δ has different $f_\delta(\delta)$ under different circumstances or at different times, the average *PCI* at the right most column will also be close to that when $f_\delta(\delta)$ is uniform.

The above discussions show that the probability distribution of δ has some, but quite limited, influence on the relative performance of the control charts and, therefore, designing control charts based on a uniform distribution is a viable design practice.

Table 2
Effect of the probability distribution of δ (τ=740, δ_{max}=4).

	Uniform	Beta		
		Skew to right (a=2, b=4)	Symmetrical (a=b=3)	Skew to left (a=4, b=2)
AEQL				
Basic $\bar{x}$	16.5153	11.0699	13.5982	19.6084
Optimal $\bar{x}$	13.8385	13.3216	11.9419	13.2512
VSSI $\bar{x}$	11.0411	10.5211	8.8610	10.1756
Basic CUSUM	11.5658	10.9260	11.2765	12.2855
Optimal CUSUM	10.6298	9.8356	10.2953	11.3009
VSSI CUSUM	6.6370	5.2405	6.0800	7.5722
Basic SPRT	9.0738	5.0826	8.0077	12.0306
Optimal SPRT	5.2821	4.0413	4.5856	5.9182
VSI SPRT	5.1795	3.9259	4.4818	5.8294

	Uniform	Beta			Average
		Skew to right	Symmetrical	Skew to left	
PCI					
Basic $\bar{x}$	3.1886 (9)	2.8197 (8)	3.0341 (9)	3.3637 (9)	3.0725 (9)
Optimal $\bar{x}$	2.6718 (8)	3.3933 (9)	2.6646 (8)	2.2732 (8)	2.7770 (8)
VSSI $\bar{x}$	2.1317 (6)	2.6800 (6)	1.9771 (5)	1.7456 (4)	2.1342 (5)
Basic CUSUM	2.2330 (7)	2.7831 (7)	2.5161 (7)	2.1075 (7)	2.4689 (7)
Optimal CUSUM	2.0523 (5)	2.5053 (5)	2.2972 (6)	1.9386 (5)	2.2470 (6)
VSSI CUSUM	1.2814 (3)	1.3349 (4)	1.3566 (3)	1.2990 (3)	1.3302 (3)
Basic SPRT	1.7519 (4)	1.2946 (3)	1.7867 (4)	2.0638 (6)	1.7151 (4)
optimal SPRT	1.0198 (2)	1.0294 (2)	1.0232 (2)	1.0152 (2)	1.0226 (2)
VSI SPRT	1.0000 (1)	1.0000 (1)	1.0000 (1)	1.0000 (1)	1.0000 (1)

Usually, if a chart designed by using a uniform $f_\delta(\delta)$ has a better (or worse) performance compared to other charts, it also has better (or worse) performance under different non-uniform $f_\delta(\delta)$.

Some SPC practitioners may have some idea regarding the shape of the probability distribution $f_\delta(\delta)$ in a particular process. For example, they may believe that $f_\delta(\delta)$ tends to be skewed to right (or left). Then, a further question is whether the optimal design for a chart is heavily or only slightly dependent on the choice of $f_\delta(\delta)$. Wu et al. (2010) study the optimization designs of several CUSUM charts based on the real probability distribution $f_\delta(\delta)$. That is, during the optimization designs, the objective function *AEQL* is calculated by Eq. (8) instead of Eq. (9). Their results show that none of the charts that is designed based on the real distribution $f_\delta(\delta)$ can bring about notable improvement in terms of *AEQL* compared with the counterpart chart designed based on a uniform distribution. For example, suppose that δ follows a beta distribution that is skewed to the left (a=2, b=4). A CUSUM chart designed based on this real shift distribution has k=1.8500 and *AEQL*=33.3977. On the other hand, a CUSUM chart designed based on a uniform distribution has k=1.6500 and *AEQL*=33.5110. This can be seen that, even though the design based on the real shift distribution has changed the optimal value of k considerably, it reduces *AEQL* only slightly (by 0.34%). The reason may be that the *AEQL* value is nearly constant within a wide range around the optimal design point. As a result, it seems that the choice of $f_\delta(\delta)$ does not have much effect on the optimal design of a chart and it is reasonable to conduct the optimal design based on a uniform distribution.

5. A factorial experiment

Next, a factorial experiment is carried out in order to further study and compare the performance of the nine charts. Three factors will be considered including the two specifications τ and δ_{max}, and the parameters of the probability distribution $f_\delta(\delta)$ of mean shift δ. Each of these factors will be studied in two levels

τ : 400,1200

$\delta_{\max}$: 2,6

$f_\delta(\delta)$: ($a=2, b=4$, skew to right),($a=4, b=2$, skew to left)

It results in eight different cases or combinations of the three factors. The general case discussed in the last section is nearly at the center of this experiment space.

The data (the *PCI* values) obtained from this experiment are displayed in Table 3. As before these *PCI* values are calculated for each case or under each column. For example, for the first case or under the leftmost column, the *AEQL* value of each chart is first determined under (τ=400, δ_{max}=2, (a=2, b=4)). Since the VSI SPRT chart has the smallest *AEQL* in this case, then the *PCI* value of each chart is obtained by dividing its *AEQL* by the *AEQL* of the VSI SPRT chart. Here, a *PCI* value again indicates the *AEQL* value of a chart relative to the *AEQL* value of the best chart when both charts are designed under the same τ and δ_{max} and applied to the process with the same $f_\delta(\delta)$. In this factorial experiment, the VSI SPRT chart usually outdoes all other charts in terms of *AEQL* under different cases. However, the optimal SPRT chart is also very competitive and always has an *AEQL* value very close to that of the VSI SPRT chart. Especially in cases 4 and 8, the *AEQL* of the optimal SPRT is slightly smaller than that of the VSI SPRT chart. In these two cases, $PCI=AEQL/AEQL_{optimal\ SPRT}$, as the best chart here is the optimal SPRT chart rather than the VSI SPRT chart.

The rightmost two columns in Table 3 display the sample mean $\overline{PCI}$ and sample standard deviation S_{PCI} of the *PCI* values of each chart over the eight cases. The sample mean $\overline{PCI}$ is the most holistic measure of the effectiveness of a chart, considering not only different specifications τ and δ_{max} but also various probability distributions $f_\delta(\delta)$ of the mean shift δ. Here, the average of *PCI*, rather than the average of *AEQL*, of each chart is considered, because the average of *AEQL* is biased to the cases in which the *AEQL* values are generally larger (e.g., when δ_{max} is larger and/or when $f_\delta(\delta)$ is skewed to left). According to $\overline{PCI}$, the charts are

Table 3
PCI values of the charts in a factorial experiment.

Chart	$\tau=400$				$\tau=1200$				$\overline{PCI}$	S_{PCI}
	$\delta_{max}=2$		$\delta_{max}=6$		$\delta_{max}=2$		$\delta_{max}=6$			
	$a=2$ $b=4$ Case 1	$a=4$ $b=2$ Case 2	$a=2$ $b=4$ Case 3	$a=4$ $b=2$ Case 4	$a=2$ $b=4$ Case 5	$a=4$ $b=2$ Case 6	$a=2$ $b=4$ Case 7	$a=4$ $b=2$ Case 8		
Basic $\bar{x}$	2.9858	2.4901	2.8118	4.2490	5.2780	3.1858	3.0294	4.2196	3.5312	0.9495
Optimal $\bar{x}$	2.7122	2.5183	3.4175	1.2212	3.7999	3.0056	3.4266	1.8351	2.7420	0.8701
VSSI $\bar{x}$	2.0447	1.8972	2.2488	1.1011	2.8178	2.1955	2.3665	1.8755	2.0684	0.4931
Basic CUSUM	2.5641	2.7367	2.0699	1.1360	3.3807	3.2411	2.6928	1.2966	2.3897	0.8297
Optimal CUSUM	2.2307	2.3857	1.8988	1.1852	2.8558	2.7805	2.3805	1.4110	2.1410	0.6036
VSSI CUSUM	1.3560	1.3969	1.2097	1.0719	1.4779	1.4681	1.2899	1.1322	1.3003	0.1516
Basic SPRT	1.0466	1.4568	1.6566	2.5599	1.0599	1.4260	1.5863	2.5399	1.6665	0.5882
Optimal SPRT	1.0193	1.0151	1.0342	1.0000	1.0467	1.0057	1.0454	1.0000	1.0208	0.0192
VSI SPRT	1.0000	1.0000	1.0000	1.0097	1.0000	1.0000	1.0000	1.0112	1.0026	0.0049

ranked as follows:

VSI SPRT, optimal SPRT, VSSI CUSUM, basic SPRT, VSSI $\overline{X}$
optimal CUSUM,
basic CUSUM, optimal $\overline{X}$,basic $\overline{X}$ chart. (19)

This is nearly the same as the ranking in Eq. (17) found for the general case in the last section, with the only exception that the optimal CUSUM chart and the VSSI $\overline{X}$ chart swap the positions.

The sample standard deviation S_{PCI} is a measure of the variability of the *PCI* values of a chart under different cases. If a chart has a smaller S_{PCI}, its *PCI* value will vary less under different situations, and this chart is more desirable in sense of performance robustness. For example, the S_{PCI} of the optimal SPRT chart is very small, and then the *PCI* values of this chart are always equal or very close to one. Contrarily, the basic $\overline{X}$ chart has a very large S_{PCI}, thus its *PCI* value is relatively small for some cases (e.g., 2.4901 in case 2) and becomes extremely large for other cases (e.g., 5.2780 in case 5). This reveals that the degree of the inferiority of the basic $\overline{X}$ chart to the best chart or other charts alters severely under different conditions. It is an undesirable feature.

Fig. 3(*a*) illustrates the $\overline{PCI}$ values of the nine charts. It clearly shows that the SPRT type charts outperform the CUSUM type charts and the latter outdo the $\overline{X}$ type charts. The grand average $\overline{\overline{PCI}}_{SPRT}$ of the SPRT type charts (i.e., the average of the $\overline{PCI}$ values of the basic SPRT, optimal SPRT and VSI SPRT charts) is equal to 1.2300. Similarly, the grand average $\overline{\overline{PCI}}_{CUSUM}$ is 1.9437 for the CUSUM type charts and $\overline{\overline{PCI}}_{\overline{X}}$ is 2.7805 for the $\overline{X}$ type charts. This indicates that, from an overall viewpoint, the SPRT chart is more effective than the CUSUM and $\overline{X}$ charts by 58% and 126%, respectively. Within each type, the FA version outperforms the optimal version and the latter surpasses the basic version. The grand averages of the *PCI* values for the FA, optimal and basic versions are $\overline{\overline{PCI}}_{adaptive}=1.4571$, $\overline{\overline{PCI}}_{optimal}=1.9680$ and $\overline{\overline{PCI}}_{basic}=2.5291$. This reveals that the FA chart outperforms the optimal chart and basic chart by 35% and 74%, respectively.

Fig. 3(*b*) illustrates the S_{PCI} values of the nine charts. Surprisingly, the patterns and characteristics of Fig. 3(*b*) is very much the same as that of Fig. 3(*a*). It means that if a type or a version of charts have higher detection effectiveness, they will also have higher performance robustness. This shows a double benefit that can be gained by using more advanced control charts.

The τ values of 400 and 1200 used in the factorial experiment are selected according to the common practice in SPC. However, in some applications, much smaller or larger τ value may have to be taken into consideration for the chart design and evaluation. In order to acquire more insight of the effect of τ on the overall performance of the control charts, the nine charts are further designed and compared by using three different τ values of 100, 740 and 5000. The value of δ_{max} is fixed as 4 for all three cases. It is noted that case 2 with ($\tau=740$) is the general case in (15).

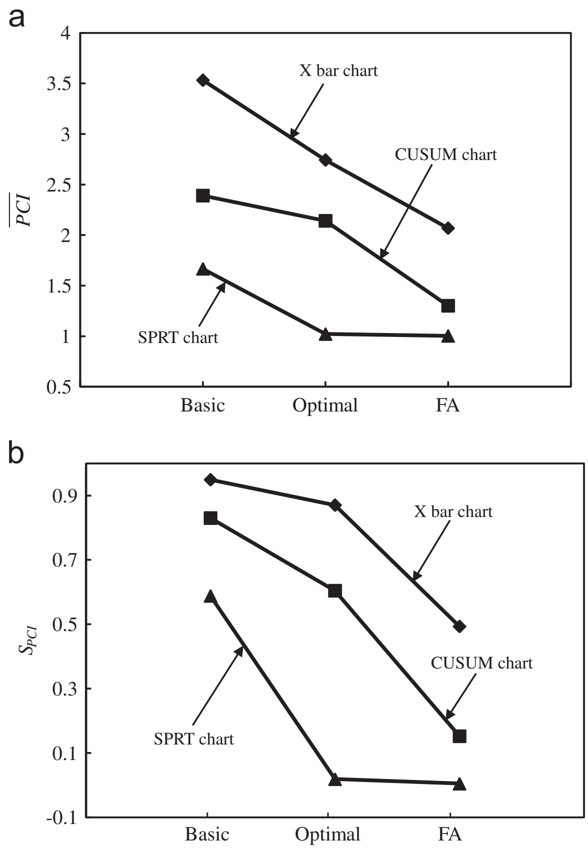

Fig. 3. Overall comparison of the nine charts.

The resultant *AEQL* values are displayed in the top half of Table 4. The bottom half of this table shows the *PCI* values for each case. The numbers inside the parentheses indicate the rankings of the *PCI* values in each case or column. It is found that the ranks for ($\tau=100$) and ($\tau=5000$) are quite similar to the ranking for ($\tau=740$) with only one or two exchanges of the ranking positions. Specifically, as shown in Fig. 3(*a*), the VSI and optimal SPRT charts are always the two most effective charts, and the optimal CUSUM chart is consistently the best FSSI chart.

Table 4
Effect of τ ($\delta_{\max}$=4).

	AEQL		
	τ=100	τ=740	τ=5000
Basic $\bar{x}$	14.0442	16.5153	25.0768
Optimal $\bar{x}$	7.6535	13.8385	25.0768
VSSI $\bar{x}$	6.0614	11.0411	20.4194
Basic CUSUM	6.4842	11.5658	19.0516
Optimal CUSUM	6.4724	10.6298	16.1194
VSSI CUSUM	5.1008	6.6370	8.3825
Basic SPRT	8.6478	9.0738	9.3382
Optimal SPRT	4.5980	5.2821	5.8848
VSI SPRT	4.5130	5.1795	5.7254
	PCI		
	τ=100	τ=740	τ=5000
Basic $\bar{x}$	3.1119 (9)	3.1886 (9)	4.3799 (9)
optimal $\bar{x}$	1.6959 (7)	2.6718 (8)	4.3799 (8)
VSSI $\bar{x}$	1.3431 (4)	2.1317 (6)	3.5665 (7)
Basic CUSUM	1.4368 (6)	2.2330 (7)	3.3276 (6)
Optimal CUSUM	1.4342 (5)	2.0523 (5)	2.8154 (5)
VSSI CUSUM	1.1302 (3)	1.2814 (3)	1.4641 (3)
Basic SPRT	1.9162 (8)	1.7519 (4)	1.6310 (4)
Optimal SPRT	1.0188 (2)	1.0198 (2)	1.0278 (2)
VSI SPRT	1.0000 (1)	1.0000 (1)	1.0000 (1)

The results of this test convince that the value of τ does not have much effect on the ranking of the charts.

6. Design tables

The earlier discussions highlight the importance of properly selecting and designing a control chart for a SPC application. This section provides three design tables (Tables 5–7) for three specified values of τ (τ=400, 740 and 1200). Inside each table, δ_{max} is specified at three levels (δ_{max}=2, 4 and 6). The users can select a chart for which the tabulated values of τ and δ_{max} are closest to the desired values for their application. These three design tables should cover many applications in SPC practice.

For each set of specified τ and δ_{max}, only the charting parameters of the optimal and FA versions of the control charts are listed. The basic versions are not recommended, because they are substantially less effective and robust than the optimal versions. Moreover, the implementation of a basic chart is in no way easier than that of a corresponding optimal chart as the optimization design only changes the values of the charting parameters.

The Average Sample Number (*ASN*) is also displayed for each SPRT chart. It provides the information of the average

Table 5
Design table (τ=400).

$\delta_{\max}$	Chart	n_1	n_2	d_1	d_2	k	g	w	H	ASN	PCI_R	PCI_S	PCI_L	PCI_{AVE}
2	Optimal $\bar{x}$	6	–	6.0000	–	–	–	–	0.8859	–	2.7122	2.6648	2.5183	2.6318
	VSSI $\bar{x}$	4	4	5.1662	0.3000	–	–	0.3429	1.1620	–	2.0447	1.9100	1.8972	1.9506
	Optimal CUSUM	5	–	5.0000	–	0.4000	–	–	0.7153	–	2.2307	2.4039	2.3857	2.3401
	VSSI CUSUM	1	2	1.8500	0.3000	0.4419	–	0.4468	2.9318	–	1.3560	1.3911	1.3969	1.3813
	Optimal SPRT	–	–	2.0500	–	0.4000	0.0679	–	4.9591	2.0505	1.0193	1.0085	1.0151	1.0143
	VSI SPRT	–	–	2.0000	0.4257	0.3419	0.4704	0.4000	5.4665	1.7226	1.0000	1.0000	1.0000	1.0000
4	Optimal $\bar{x}$	2	–	2.0000	–	–	–	–	1.8214	–	3.2923	2.4917	1.8654	2.5498
	VSSI $\bar{x}$	2	2	2.3338	0.3000	–	–	0.6816	1.8208	–	2.1290	1.7697	1.6887	1.8625
	Optimal CUSUM	2	–	2.0000	–	0.6338	–	–	1.4803	–	2.1397	2.0644	1.8379	2.0140
	VSSI CUSUM	1	2	1.3338	0.3000	0.6000	–	0.7482	2.6132	–	1.2840	1.2933	1.2495	1.2756
	Optimal SPRT	–	–	1.3419	–	0.5000	0.5707	–	4.0534	1.3464	1.0000	1.0101	1.0281	1.0127
	VSI SPRT	–	–	1.3419	0.7419	0.4500	0.8221	0.7162	4.2440	1.2564	1.0125	1.0000	1.0000	1.0042
6	Optimal $\bar{x}$	1	–	1.0000	–	–	–	–	2.8070	–	3.4175	2.0063	1.2212	2.2150
	VSSI $\bar{x}$	1	1	1.1838	0.3000	–	–	0.7956	2.8076	–	2.2488	1.4264	1.1011	1.5921
	Optimal CUSUM	1	–	1.0000	–	0.9500	–	–	2.3320	–	1.8988	1.5316	1.1852	1.5385
	VSSI CUSUM	1	2	1.1338	0.3000	0.7081	–	1.1011	2.5283	–	1.2097	1.1545	1.0719	1.1454
	Optimal SPRT	–	–	1.1338	–	0.6581	0.7807	–	3.1191	1.1381	1.0342	1.0000	1.0000	1.0114
	VSI SPRT	–	–	1.1838	0.7419	0.4500	1.1308	0.9068	3.9498	1.1314	1.0000	1.0025	1.0097	1.0041

Table 6
Design table (τ=740).

$\delta_{\max}$	Chart	n_1	n_2	d_1	d_2	k	g	w	H	ASN	PCI_R	PCI_S	PCI_L	PCI_{AVE}
2	Optimal $\bar{x}$	7	0	7	–	–	–	–	0.8871	–	3.2605	3.0304	2.7798	3.0236
	VSSI $\bar{x}$	4	4	5.5919	0.3000	–	–	0.2568	1.2738	–	2.5233	2.1419	2.0038	2.2230
	Optimal CUSUM	5	0	5.0000	–	0.4000	–	–	0.8651	–	2.5720	2.7047	2.6172	2.6313
	VSSI CUSUM	1	2	1.9743	0.3000	0.3919	–	0.4972	3.5447	–	1.3677	1.4190	1.4549	1.4139
	Optimal SPRT	–	–	2.1581	–	0.3419	0.1709	–	6.4181	2.1627	1.0000	1.0008	1.0283	1.0097
	VSI SPRT	–	–	2.0081	0.3757	0.2919	0.6072	0.4500	7.0177	1.7459	1.0033	1.0000	1.0000	1.0011
4	Optimal $\bar{x}$	3	0	3.0000	–	–	–	–	1.5286	–	3.3933	2.6646	2.2732	2.7770
	VSSI $\bar{x}$	2	2	2.4419	0.3000	–	–	0.5762	1.9666	–	2.6799	1.9771	1.7456	2.1342
	Optimal CUSUM	2	0	2.0000	–	0.6838	–	–	1.5917	–	2.5053	2.2972	1.9386	2.2470
	VSSI CUSUM	1	2	1.3419	0.3000	0.5500	–	0.8769	3.0916	–	1.3349	1.3566	1.2990	1.3302
	optimal SPRT	–	–	1.3419	–	0.4500	0.6928	–	5.0004	1.3425	1.0294	1.0232	1.0152	1.0226
	VSI SPRT	–	–	1.3919	0.6419	0.4000	0.8790	0.7243	5.3416	1.2909	1.0000	1.0000	1.0000	1.0000
6	Optimal $\bar{x}$	2	0	2.0000	–	–	–	–	1.9670	–	2.8722	2.0619	1.7941	2.2427
	VSSI $\bar{x}$	1	1	1.2919	0.3000	–	–	0.5329	3.0000	–	2.9443	1.6706	1.2000	1.9383
	Optimal CUSUM	1	0	1.0000	–	0.9500	–	–	2.6509	–	2.1942	1.7186	1.2940	1.7356
	VSSI CUSUM	1	2	1.1338	0.3000	0.6581	–	1.2672	2.9721	–	1.2730	1.2076	1.1027	1.1944
	Optimal SPRT	–	–	1.1838	–	0.5500	0.8229	–	4.1604	1.1882	1.0000	1.0088	1.0273	1.0120
	VSI SPRT	–	–	1.1838	0.7419	0.4500	1.1651	0.9068	4.5698	1.1300	1.0232	1.0000	1.0000	1.0077

Table 7
Design table ($\tau=1200$).

δ_{max}	Chart	n_1	n_2	d_1	d_2	k	g	w	H	ASN	PCI_R	PCI_S	PCI_L	PCI_{AVE}
2	Optimal $\bar{x}$	8	0	8.0000	–	–	–	–	0.8750	–	3.7999	3.4091	3.0056	3.4049
	VSSI $\bar{x}$	5	5	6.6500	0.3000	–	–	0.2850	1.1794	–	2.8178	2.3416	2.1955	2.4517
	Optimal CUSUM	6	0	6.0000	–	0.3919	–	–	0.7979	–	2.8558	2.9593	2.7805	2.8652
	VSSI CUSUM	1	2	1.8500	0.3000	0.3919	–	0.6306	3.9189	–	1.4779	1.4906	1.4681	1.4788
	Optimal SPRT	–	–	2.1581	–	0.3419	0.1851	–	7.1053	2.1606	1.0467	1.0149	1.0057	1.0224
	VSI SPRT	–	–	2.2581	0.3757	0.2919	0.5248	0.3500	7.8742	1.8727	1.0000	1.0000	1.0000	1.0000
4	Optimal $\bar{x}$	3	0	3.0000	–	–	–	–	1.6206	–	4.2193	2.9484	2.3118	3.1598
	VSSI $\bar{x}$	2	2	2.6500	0.3000	–	–	0.4190	2.0750	–	3.1906	2.1523	1.8439	2.3956
	Optimal CUSUM	2	0	2.0000	–	0.6838	–	–	1.7655	–	2.7835	2.4621	2.0492	2.4316
	VSSI CUSUM	1	2	1.3500	0.3000	0.5081	–	1.0141	3.5403	–	1.3773	1.3974	1.3472	1.3740
	Optimal SPRT	–	–	1.3419	–	0.4000	0.8039	–	5.9984	1.3444	1.0364	1.0131	1.0010	1.0169
	VSI SPRT	–	–	1.3919	0.7419	0.3500	0.9199	0.8743	6.5433	1.3393	1.0000	1.0000	1.0000	1.0000
6	Optimal $\bar{x}$	2	0	2.0000	–	–	–	–	2.0755	–	3.4266	2.2357	1.8351	2.4991
	VSSI $\bar{x}$	2	2	2.2081	0.3000	–	–	0.8672	2.0753	–	2.3665	1.8867	1.8755	2.0429
	Optimal CUSUM	1	0	1.0000	–	0.9500	–	–	2.9033	–	2.3805	1.8726	1.4110	1.8880
	VSSI CUSUM	1	2	1.1338	0.3000	0.6581	–	1.2828	3.1827	–	1.2899	1.2343	1.1322	1.2188
	Optimal SPRT	–	–	1.1338	–	0.5000	1.0683	–	4.7723	1.1378	1.0454	1.00554	1.0000	1.0170
	VSI SPRT	–	–	1.1838	0.6419	0.4000	1.2501	1.0568	5.4789	1.1365	1.0000	1.0000	1.0112	1.0037

sample size. But *ASN* is not a charting parameter and is not needed for operating a SPRT chart.

As aforementioned, the sampling intervals, as well as the specification τ, in the design tables are expressed in terms of a time unit equal to the time period in which the available resource allows one product to be inspected. This setting will be further explained in the next section of the example.

From the design tables, it is found that the optimal sample sizes of all control charts increase along with the increase of τ and/or the decrease of δ_{max}. Specifically, the optimal sample sizes are often quite different from the conventional settings. For example, the sample sizes $n_{\bar{X}}$ of the optimal $\bar{X}$ charts are equal to 1 or 2 when $\delta_{max}=6$ (compared with $4 \le n_{\bar{X}} \le 6$ by convention) and the sample sizes n_{CUSUM} of the optimal CUSUM charts are equal to 5 or 6 when $\delta_{max}=2$ (compared with the commonly recommended value of $n_{CUSUM}=1$).

It is also noted that the two sample sizes n_1 and n_2 of a VSSI $\bar{X}$ chart are always the same. This means that a VSI $\bar{X}$ chart is actually as effective as a VSSI $\bar{X}$ chart. For any $\bar{X}$ chart, there may be an optimal sample size which is very critical to the overall performance of the $\bar{X}$ chart. The deviation of either n_1 or n_2 of a VSSI $\bar{X}$ chart from this optimal value may result in the increase of *AEQL*.

The rightmost four columns in each design table enumerate the values of PCI_R, PCI_S, PCI_L and PCI_{AVE} for each chart. Here, PCI_R carries the *PCI* value of the chart when the real probability distribution of δ is a beta distribution skew to right. Similarly, PCI_S or PCI_L is related to the beta distribution that is symmetrical or skew to left. Finally, PCI_{AVE} is the average of PCI_R, PCI_S and PCI_L. The data related to the variability of *PCI* (e.g., S_{PCI} in Table 3) have not been listed, because, as found earlier, the robustness of a chart is usually positively correlated with its effectiveness.

Usually, the users are not aware of the accurate distribution of δ. However, they may have some general and rough idea about it. For example, they may tell that most of the mean shifts cluster to the lower end, that is, having a distribution skew to right. Under such circumstance, they may make use of the data under the column of PCI_R. On the other hand, if the users have no idea at all about the distribution of δ, they can refer to PCI_S or PCI_{AVE}. The latter takes all different distributions into consideration.

In addition to effectiveness and robustness, simplicity in implementation is also an important consideration when selecting a control chart. The adaptive charts (the VSSI $\bar{X}$, VSSI CUSUM, optimal SPRT and VSI SPRT charts) generally have better overall performance than the FSSI charts (the optimal $\bar{X}$ and optimal CUSUM charts), because these adaptive charts allow the sampling rate to vary at each sampling point. However, it will in turn increase the difficulty to run the charts. This operational complexity cannot be overcome just by means of a computer, because the changes of sample sizes and sampling intervals must be carried out by the operators or an automatic inspection system. Among the four adaptive charts, the implementation of the optimal SPRT chart is relatively easier, because this chart uses a fixed sampling interval and only adapts the sample size. On the other hand, the FSSI charts use fixed sample size and sampling interval, therefore they are simpler for operation. The optimal $\bar{X}$ chart is especially easy for implementation. However, if a computer-aided SPC system is in use, there is almost no difference in the difficulty of running the two FSSI charts (i.e., the optimal $\bar{X}$ and optimal CUSUM charts).

The four types of *PCI* in the design tables facilitate the users to consider both effectiveness of performance and simplicity in operation when selecting a chart. If the *PCI* value shows that the improvement gained by a complicated chart in effectiveness and robustness is insignificant, it may not be worthwhile to replace a simpler chart by this complicated one. On the contrary, if the achievable improvement in terms of *PCI* is substantial, the users may believe that the gain in effectiveness and robustness should be sufficient to outweigh the increase in complexity.

As a general guideline, the optimal CUSUM chart and optimal SPRT chart are recommended for most of the SPC applications. Considering the difference in the difficulty of implementation, the optimal CUSUM chart is selected for the FSSI charts when the users prefer to using fixed sample size and sampling interval, and the optimal SPRT chart for the adaptive charts when detecting speed is critical and the users would like to adopt adaptive feature for better performance. The optimal CUSUM chart is the most effective and robust FSSI chart and can be implemented as easily as the optimal $\bar{X}$ chart when an on-site computer is available. The optimal SPRT chart may be the best choice among the adaptive charts. This chart is almost as effective and robust as the VSI SPRT chart and is much better than the VSSI $\bar{X}$ and VSSI CUSUM charts. Meanwhile, the optimal SPRT chart enjoys the ease of using a fixed sampling interval. All other three adaptive charts (i.e., the VSSI $\bar{X}$, VSSI CUSUM and VSI SPRT charts) have to change both sample sizes and sampling intervals during the operation. Some SPC users or researchers may not be familiar with the SPRT chart. However, taking both performance and simplicity into consideration, it is strongly recommended that the VSSI $\bar{X}$ and VSSI CUSUM charts can be replaced by the optimal SPRT chart in all applications of the adaptive charts.

7. An example

An illustrative example is shown in this section (Wu et al., 2009). A manufacturing factory produces a type of shaft for an aero-engine. The diameter x of the shaft is a key dimension. An upper-sided control chart will be adopted to detect the increasing mean shift of x. The nominal value and tolerance of x are specified as 65 ± 0.009 mm. From pilot runs it is found that the probability distribution of x is approximately normal and the in-control standard deviation σ_0 is estimated to be 0.0015 mm. The in-control mean μ_0 can be easily adjusted to the nominal value of 65 mm (i.e., the center between the specification limits). In order to standardize the design and operation, the diameter x is converted to z conforming to a standard normal distribution when the process is in control.

$$z = \frac{x-65}{0.0015}.$$

The inspection rate is set as one unit/h and thus the time unit is equal to one hour or 60 min. The in-control ATS_0 is specified as 700 h by the Quality Assurance (QA) engineer. The QA engineer is interested to study the chart performance in a mean shift range ($0<\delta \le 4$), i.e., $\delta_{max}=4$. Based on the above specifications, a design can be selected from Table 6 (where τ is equal to 740, close to 700) and within the catalog of ($\delta_{max}=4$). Since the QA engineer has no idea about the probability distribution of the mean shift δ, he checks PCL_{AVE} to figure out the effectiveness and robustness of the control charts. The PCL_{AVE} values show that the optimal SPRT chart is only about 2% less effective than the most effective VSI SPRT chart. Furthermore, the former uses a fixed sampling interval and thus can reduce some operational difficulty. The QA engineering finally decides to adopt the optimal SPRT chart for monitoring the mean of the diameter. The parameters (sampling interval d, reference parameter k, lower control limit g and upper control limit H) of this optimal SPRT chart can be picked up from Table 6 and listed below, together with the resultant ASN, ATS_0 and inspection rate r_0.

$$d=1.3419, k=0.4500, g=0.6928, H=5.0004, ASN=1.3425, ATS_0=740, r_0=1.$$

It is noted that the sampling interval $d=1.3419\times 60=80.5140$ min. In order to facilitate the implementation, d is rounded off to 80 min. This adjustment will change the value of ATS_0 to 734 (0.81% smaller than the original value of 740) and increase the value of r_0 to 1.0069 (0.69% larger). Both changes are minor and tolerable.

To run this optimal SPRT chart, one sample is inspected for every 80 min. The sample size varies, but its average is equal to 1.3425. In each sample of the optimal SPRT chart, the statistic C_i is updated based on each observed z_i.

$$C_0 = 0,$$
$$C_i = C_{i-1} + z_i - k.$$

If $C_i > H$, an increasing mean shift is signaled. On the other hand, if C_i is smaller than g, the process is thought in control. For other circumstances, sampling will be continued.

Fig. 4 displays the ATS curve of this optimal SPRT chart. Also presented are the ATS curves of the VSSI $\bar{X}$ and VSSI CUSUM charts for the purpose of comparison. Fig. 4(a) shows the ATS curves over the whole shift range except for very minor δ. When ($\delta=0$), the in-control ATS_0 values of all charts are very close to τ. Fig. 4(b) zooms in the ATS curves under moderate and large mean shifts. It can be seen that the optimal SPRT chart consistently produces smaller out-of-control ATS values over the entire mean shift range compared with other two charts. The two ratios of ($AEQL_{VSSI\_\bar{X}}$/$AEQL_{optimal\_SPRT}$) and ($AEQL_{VSSI\_cusum}$/$AEQL_{optimal\_SPRT}$) are equal to 2.1037 and 1.2646, respectively. This means that the average speed of the optimal SPRT chart for detecting out-of-control cases is higher than that of the VSSI $\bar{X}$ and VSSI CUSUM charts by 110% and 26%, respectively. Meanwhile the optimal SPRT chart is easier for implementation as it uses fixed sampling interval.

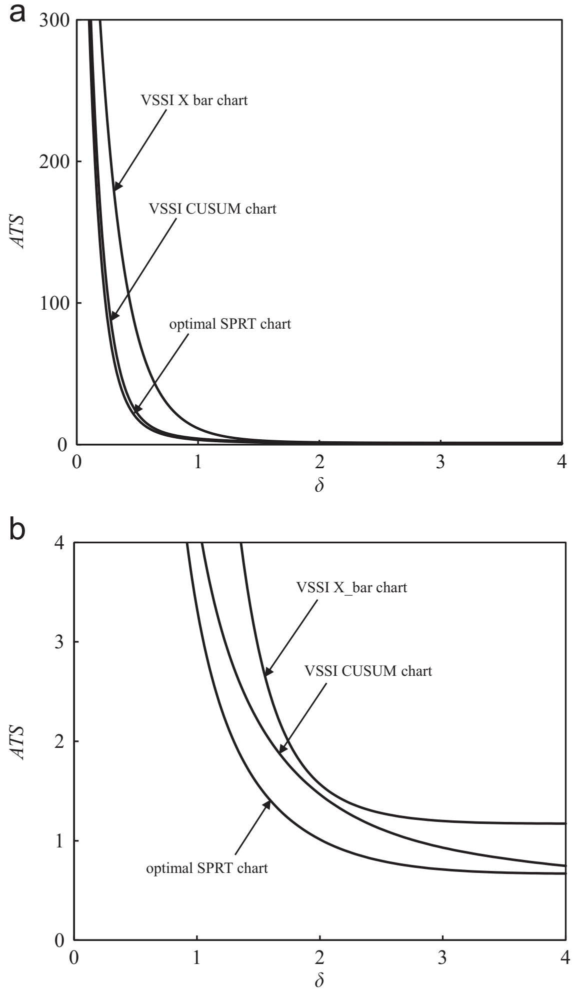

Fig. 4. Example.

8. Discussions and conclusions

This article carries out a systematic comparison among three main types of control charts ($\bar{X}$, CUSUM and SPRT charts), each with three versions (basic, optimal and fully adaptive (FA) versions), for monitoring process mean. The comparisons are conducted under various conditions, including not only different in-control ATS_0 and mean shift ranges, but also various probability distributions of mean shift δ. A Performance Comparison Index, PCI, is proposed as the measure of the relative overall performance of the charts.

This study ranks the charts in line of both types and versions according to detection effectiveness and performance robustness. It gives the quantitative evaluation of the superiority of one chart compared with others. Such information will facilitate the users to select a chart based on both superiority in performance and simplicity in implementation. By summing up all the results, the optimal CUSUM and optimal SPRT charts are recommended as the best FSSI and adaptive charts, respectively. One may even get some general idea about the relative performance of many other charts by referring to the nine charts studied in this article. For example, the performance of a VSI CUSUM chart must be between the optimal CUSUM chart and the VSSI CUSUM chart.

Both the optimal and adaptive charts are designed by an optimization procedure using Average Extra Quadratic Loss (*AEQL*) as the objective function. The optimization design of the control charts is strongly recommended, as it can significantly improve the overall performance of the charts and meanwhile does not increase the difficulty in implementation. The optimal values of many charting parameters (e.g., the sample sizes of the $\overline{X}$ and CUSUM charts) may be far different from the ones based on the common conventions.

The comparison of performance robustness is first discussed in this study. It is found that the ranking of the charts on robustness is usually the same as the ranking on effectiveness. The more effective charts also have more stable performance under different conditions.

This study also provides several design tables containing 54 charts for different design specifications. These tables will aid the users to select a chart by considering both performance and simplicity in implementation, as well as the probability distribution of mean shift δ.

In this study, the Average Extra Quadratic Loss (*AEQL*) and Average Ratio of *ATS* (*ARATS*) are used to evaluate the overall effectiveness of the control charts. Both give similar results. If other alternative measures are employed, the numerical results may be somewhat different, but the general conclusions pertaining to the performance comparison of charts should be similar.

This study is conducted based on some general assumptions and conventions, such as the known in-control mean μ_0 and standard deviation σ_0, and the normal distribution of x. It is interesting to carry out further studies on how the performance comparison will be affected when μ_0 and σ_0 are estimated, or when the quality characteristic follows a non-normal distribution or is correlated. Furthermore, a more systematic investigation should be conducted to study the effect of the probability distribution of the mean shift δ on the optimization designs of all the control charts.

Probably, the most interesting extension of this study is to evaluate and compare the performance of the control charts for detecting two-sided mean shifts of a variable or shifts in both mean and variance. The optimization designs of these charts are more difficult, because the properties of these charts cannot be easily obtained from the properties of the individual one-sided charts and their optimal charting parameters are different from the optimal parameters of the one-sided charts. Due to the limitation on the length of an article, all these issues will be pursued in the future works.

References

Arnold, J.C., Reynolds, M.R.J.R., 2001. CUSUM control charts with variable sample sizes and sampling intervals. Journal of Quality Technology 33, 66–81.

Celano, G., Magalhães, M.S., De., Costa, A.F.B., Fichera, S., 2011. A stochastic shift model for economically designed charts constrained by the process stage configuration. International Journal of Production Economics 132, 315–325.

Chen, A., Chen, Y.K., 2007. Design of EWMA and CUSUM control charts subject to random shift sizes and quality impacts. IIE Transactions 39, 1127–1141.

Chou, C.Y., Chen, C.H., Liu, H.R., 2000. Economic–statistical design of $\overline{X}$ charts for non-normal data by considering quality loss. Journal of Applied Statistics 27, 939–951.

Colosimo, B.M., Pacella, M., 2010. A comparison study of control charts for statistical monitoring of functional data. International Journal of Production Research 48, 1575–1601.

Costa, A.F.B., Machado, M.A.G., 2011. Variable parameter and double sampling X-bar charts in the presence of correlation: The Markov chain approach. International Journal of Production Economics 130, 224–229.

Das, N., 2009. A comparison study of three non-parametric control charts to detect shift in location parameters. International Journal of Advanced Manufacturing Technology 41, 799–807.

Domangue, R., Patch, S.C., 1991. Some omnibus exponentially weighted moving average statistical process monitoring schemes. Technometrics 33, 299–313.

Hawkins, D.M., Olwell, D.H., 1998. Cumulative Sum Control Charts and Charting for Quality Improvement. Springer-Verlag, New York, NY.

Magalhães, M.S.D., Costa, A.F.B., Neto, F.D.M., 2009. A hierarchy of adaptive $\overline{X}$ control charts. International Journal of Production Economics 119, 271–283.

Margavio, T.M., Conerly, M.D., 1995. A comparison of multivariate moving average control charts for the process mean. International Journal of Production Research 33, 1313–1321.

Montgomery, D.C., 2009. Introduction to Statistical Quality Control. John Wiley & Sons, New York.

Ou, Y.J., Wu, Z., Chen, S.L., Lee, K.M., 2011a. An improved SPRT control chart for monitoring process mean. International Journal of Advanced Manufacturing Technology 51, 1045–1054.

Ou, Y.J., Wu, Z., Lee, K.M., Chen, S.L., 2011b. A highly effective SPRT control chart for monitoring process mean. Technical Report, School of Mechanical and Aerospace Engineering, Nanyang Technological University, Singapore.

Page, E.S., 1954. Continuous inspection schemes. Biometrika 41, 100–115.

Reynolds Jr., M.R., Stoumbos, Z.G., 2004a. Should observations be grouped for effective process monitoring? Journal of Quality Technology 36, 343–366.

Reynolds Jr., M.R., Stoumbos, Z.G., 2004b. Control charts and the efficient allocation of sampling resources. Technometrics 46, 200–214.

Reynolds Jr., M.R., Stoumbos, Z.G., 2006. Comparisons of some exponentially weighted moving average control charts for monitoring the process mean and variance. Technometrics 48, 550–567.

Reynolds Jr., M.R., Lou, J.Y., 2010. An evaluation of a GLR control chart for monitoring the process mean. Journal of Quality Technology 42, 287–310.

Runger, G.C., Montgomery, D.C., 1993. Adaptive sampling enhancements for Shewhart control charts. IIE Transactions 25, 41–51.

Ryu, J.H., Wan, H., Kim, S., 2010. Optimal design of a CUSUM chart for a mean shift of unknown size. Journal of Quality Technology 42, 311–326.

Serel, D.A., Moskowitz, H., 2008. Joint economic design of EWMA control charts for mean and variance. European Journal of Operational Research 184, 157–168.

Shewhart, W.A., 1931. Economic Control of Quality of Manufacturing Product. Van Nostrand, New York.

Shu, L., Jiang, W., 2006. A Markov chain model for the adaptive CUSUM control chart. Journal of Quality Technology 38, 135–147.

Sparks, R.S., 2000. Cusum charts for signalling varying location shifts. Journal of Quality Technology 32, 157–171.

Stoumbos, Z.G., Reynolds Jr., M.R., 1997. Control charts applying a sequential test at fixed sampling intervals. Journal of Quality Technology 29, 21–40.

Stoumbos, Z.G., Reynolds Jr., M.R., 2001. The SPRT control chart for the process mean with samples starting at fixed times. Nonlinear Analysis 2, 1–34.

Taguchi, G., Wu, Y., 1980. Introduction to Off-Line Quality Control. American Supplier Institute, Romulus, MI.

Tannock, J.D.T., 1997. An economic comparison of inspection and control charting using simulation. International Journal of Quality & Reliability Management 14, 687–699.

Wald, A., 1947. Sequential Analysis. Wiley, New York.

Woodall, W.H., Montgomery, D.C., 1999. Research issues and ideas in statistical process control. Journal of Quality Technology 31, 376–386.

Wu, Z., Shamsuzzaman, M., Pan, E.S., 2004. Optimization design of the control charts based on Taguchi's loss function and random process shifts. International Journal of Production Research 42, 379–390.

Wu, Z., Yang, M., Jiang, W., Khoo, M.B.C., 2008. Optimization designs of the combined Shewhart-CUSUM control charts. Computational Statistics and Data Analysis 53, 496–506.

Wu, Z., Jiao, J.X., Yang, M., Liu, Y., Wang, Z.J., 2009. An enhanced adaptive CUSUM control chart. IIE Transactions 41, 642–653.

Wu, Z., Yang, M., Khoo, M.B.C., Yu, F.J., 2010. Optimization designs and performance comparison of two CUSUM schemes for monitoring process shifts in mean and variance. European Journal of Operational Research 205, 136–150.

Wu, Z., Yang, M., Khoo, M.B.C., Castagliola, P., 2011. What are the best sample sizes for the Xbar and CUSUM charts? International Journal of Production Economics 131, 650–662.

Zhang, S., Wu, Z., 2006. Monitoring the process mean and variance by the WLC scheme with variable sampling intervals. IIE Transactions 38, 377–387.

Zhou, W., Lian, Z., 2011. Optimum design of a new VSS-NP chart with adjusting sampling inspection. International Journal of Production Economics 129, 8–13.